J|A|C|S
ARTICLES
Published on Web 01/23/2007

# Positive and Negative $TiO_2$ Micropatterns on Organic Polymer Substrates

Peng Yang,[†,‡] Min Yang,[†,‡,§] Shengli Zou,[†,‡] Jingyi Xie,[†,‡] and Wantai Yang*[,†,‡]

*Contribution from the State Key Laboratory of Chemical Resource Engineering, Beijing 100029, China, and Department of Polymer Science, Beijing University of Chemical Technology, P.O. Box 37, Beijing 100029, China*

Received May 27, 2006; E-mail: yangwt@mail.buct.edu.cn

***Abstract:*** Ordered titanium dioxide ($TiO_2$) films have received increasing attention because of their great potential in photocatalysis, energy conversion, and electrooptical techniques. Such films are often fabricated as coatings on various substrates such as silicon or a variety of polymers. Liquid-phase deposition (LPD) of $TiO_2$ films is especially promising for organic substrates due to its very mild reaction conditions. In the present paper, LPD is conducted on a wettability-patterned polypropylene surface to fabricate positive and negative $TiO_2$ micropatterns. A thin layer of ammonium persulfate in an aqueous solution was sandwiched between two biaxially oriented polypropylene (BOPP) films, and a photomask was employed to control the irradiation region. Within a short time interval, a high hydrophilicity could be obtained on the irradiation region, and an effective wettability contrast between the irradiated and unirradiated regions could be created to further induce the formation of two types of $TiO_2$ micropatterns. Up until now, most approaches for micropatterning have been based on self-assembled monolayers on surfaces of gold (or other noble metals), silicon, and various polyesters. With the present method, however, there is no longer any limitation in the type of substrate used. Our work demonstrates that an anatase $TiO_2$ film could be selectively deposited on a hydrophilic region, giving rise to a positive pattern with significant bonding strength and good line edge acuity, providing an effective solution toward the microfabrication on various inert polymer substrates. More surprisingly, we find, for the first time, that $TiO_2$ could also be selectively retained on a hydrophobic region to form a negative pattern by simply adjusting the reaction conditions. Further analysis of the mechanism shows that, independent of the deposition conditions, the $TiO_2$ deposition pattern changes gradually, from being initially negative to becoming positive as the deposition time increases. The surface functionality changes (from sulfate to hydroxyl groups) during the deposition, and the resulting difference in the affinity for $TiO_2$ is used to interpret this negative-to-positive pattern change. Such negative patterns refute the conventional opinion that only hydrophilic regions favor the formation of $TiO_2$ films and could be used to fabricate large areas ($mm^2$) of interconnected $TiO_2$ micronetworks. Such networks are difficult to obtain by conventional metallic masks, and the present method is expected to provide new strategies in the fabrication of flexible photomasks and macro/mesoporous $TiO_2$ films. An example is given wherein a patterned photografting of poly(acrylic acid) on the surface of BOPP is achieved by using such a polymer-based photomask. The innovativeness of this method arises from its ability to provide negative patterning, whereas present related approaches have been found only to give positive patterns from an equivalent photomask. Unlike complex photolithography procedures, our irradiation and patterning process does not require the use of positive or negative photoresists, and should thus prove to be a simple, fast, and low-cost method.

## Introduction

The deposition of titanium dioxide ($TiO_2$) on a variety of substrates has attracted a lot of attention because of its wide application in photocatalysis, photoelectric conversion, dielectrics, and nonlinear optics.[1−5] The patterning or array of $TiO_2$ on various substrates would find a direct utility in devices such as electrical elements,[4] solar cells,[6] photocatalysts,[7] sensors,[8] and so forth. Recently, the adsorption of proteins on $TiO_2$-

[†] State Key Laboratory of Chemical Resource Engineering.
[‡] Beijing University of Chemical Technology.
[§] Current address: Department of Chemical Engineering, Tsinghua University, Beijing, China.

(1) Sukharev, V.; Wold, A.; Gao, Y. M.; Dwight, K. *J. Solid State Chem.* **1995**, *119*, 339.
(2) Gratzel, M. *Nature* **1992**, *353*, 737.
(3) Tian, Z. R.; Voigt, J. A.; Liu, J.; Mckenzie, B.; Xu, H. *J. Am. Chem. Soc.* **2003**, *125*, 12384.
(4) Kovtyukhova, N. I.; Martin, B. R.; Mbindyo, J. K. N.; Mallouk, T. E.; Cabassi, M.; Mayer, T. S. *Mater. Sci. Eng., C* **2002**, *19*, 255.
(5) Linsebigler, A. L.; Lu, G.; Yates, J. T., Jr. *Chem. Rev.* **1995**, *95*, 735.
(6) Narazaki, A.; Kawaguchi, Y.; Niino, H.; Shojiya, M.; Koyo, H.; Tsunetomo, K. *Chem. Mater.* **2005**, *17*, 6651
(7) (a) Park, J. H.; Kim, S.; Bard, A. J. *Nano Lett.* **2006**, *6*, 24. (b) Morand, R.; Lopez, C.; Koudelka-Hep, M.; Kedzierzawski, P.; Augustynski, J. *J. Phys. Chem. B* **2002**, *106*, 7218.
(8) Zuruzi, A. S.; MacDonald, N. C. *Adv. Funct. Mater.* **2005**, *15*, 396.
(9) Liu, S.; Chen, A. *Langmuir* **2005**, *21*, 8409.
(10) Carbone, R.; Marangi, I.; Bongiorno, G.; Lenardi, C.; Vinati, S.; Fiorentini, F.; Pelicci, P. G.; Milani, P. *China International Conference on Nanoscience and Technology (ChinaNANO2005)*, Beijing, China, June 9−11, 2005; Technical Program, p 18.

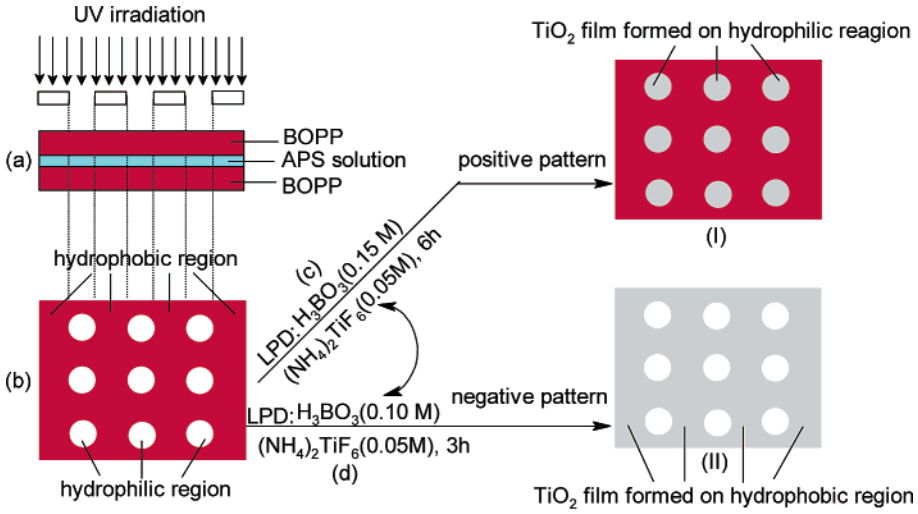


***Figure 1.*** Schematic process of $TiO_2$ micropatterning on BOPP films. (a) A thin layer of an aqueous APS solution was sandwiched between two BOPP films, and selective UV irradiation was conducted with the use of a photomask. (b) CPO took place in the irradiated region, and the resulting wettability-patterned surface was utilized to fabricate positive (I) patterns under positive conditions (c) and negative (II) patterns under negative conditions (d).

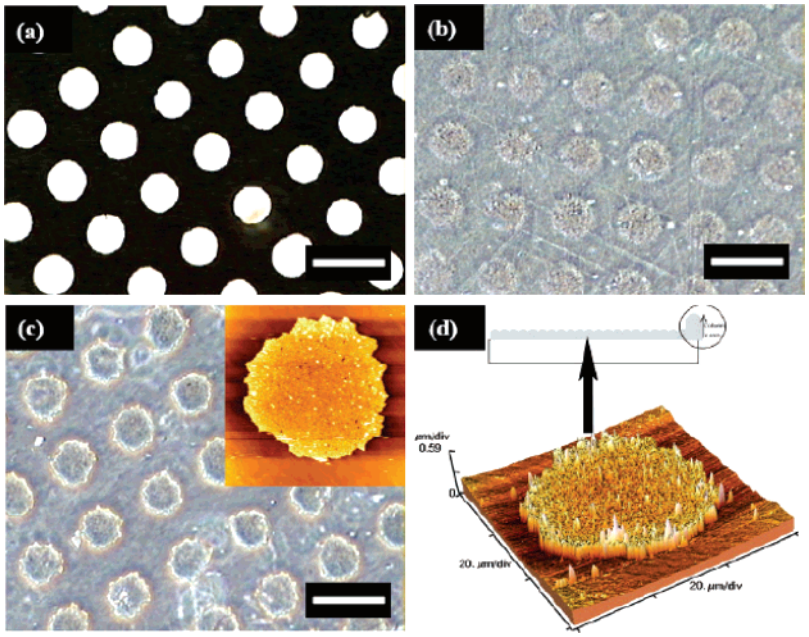


***Figure 2.*** Optical (phase contrast mode) and AFM images of positive patterns on a BOPP surface obtained under positive conditions (Figure 1c): (a) an optical image of photomask a with circular patterns; (b) an optical image of the as-deposited film; (c) an optical image of the positive pattern (the inset depicts a detailed circle of a deposited $TiO_2$ layer by AFM); (d) a 3D AFM profile image of the positive pattern and the schematic column growth of a $TiO_2$ crystalline particle along the *c* axis. This column pattern could be clearly found in the lower 3D AFM profile picture. The scale bars in images a−c are 80 $\mu$m.

patterned substrates has also been reported for biosensors[9] and protein microarray[10] applications.

Some methods, such as etching, chemical vapor deposition (CVD),[11] rapid thermal oxidation,[12] sol−gel,[13] and sputtering,[14] have been used to fabricate $TiO_2$ films on inorganic or metal substrates, including silicon wafers, fused quartz, gold-coated quartz crystal microbalances, graphite electrodes, etc. These materials are tough enough to support the stringent reaction conditions that these methods imply. In opposition, certain "weaker" and softer materials, such as polymers, require a milder method to achieve the desired pattern. An excellent approach for accomplishing this is liquid-phase deposition (LPD) at low temperatures, a method that has been developed on silicon[15−19] and polymer surfaces.[20−29] This method utilizes the hydrolysis of a soluble titanium fluoride complex ($TiF_6^{2-}$) in the presence

***Scheme 1.*** Reaction Mechanism for LPD[30−34]

$$[TiF_6]^{2-} + nH_2O \rightleftharpoons [TiF_{6-n}(OH)_n]^{2-} + nHF \quad (1)$$

$$H_3BO_3 + 4HF \rightleftharpoons HBF_4 + nH_2O \quad (2)$$

$$[TiF_{6-n}(OH)_n]^{2-} \xrightarrow{H_2O} [TiF_{5-n}(OH)_{n+1}]^{2-} \quad (3)$$

$$[TiF_{5-n}(OH)_{n+1}]^{2-} + H^+ + F^- \xrightarrow{(5-n)H_2O} [Ti(OH)_6]^{2-} + (6-n)F^- + (6-n)H^+ \quad (4)$$

$$\text{Olation: Ti-OH + Ti-OH} \longrightarrow \text{Ti-OH-Ti + } H_2O \quad (5)$$

$$\text{Oxolation: Ti-OH + Ti-OH} \longrightarrow \text{Ti-O-Ti + } H_2O \quad (6)$$

(11) Rausch, N.; Burte, E. P. *J. Electrochem. Soc.* **1993**, *140*, 145.
(12) Burnes, G. P. *J. Appl. Phys.* **1989**, *65*, 2095.
(13) Selvaraj, U.; Prasadarao, A. V.; Komarneni, S.; Roy, R. *J. Am. Chram. Soc.* **1992**, *75*, 1167.
(14) Akeuchi, M.; Itoh, I.; Nagasaka, H. *Thin Solid Films* **1978**, *51*, 83.

***Table 1.*** Features and Line Edge Variations in Various Processes

| process | | designed av line width ($\mu$m) | practical av line width ($\mu$m) | line edge variation (%) |
|---|---|---|---|---|
| photomask b (Figure 3a) | I | 50 | 50 | 1.73 |
| | II | 70 | 70 | 1.54 |
| positive pattern on BOPP surface by ultrasonic washing (Figure 3b) | | 50 | 56.068 | 17.11 |
| positive pattern on BOPP surface by adhesive peeling (Figure 3c) | | 50 | 49.208 | 4.86 |
| negative pattern on BOPP surface by ultrasonic washing (Figure 5) | | 70 | 67.231 | 1.45 |
| negative pattern on adhesive tape by adhesive peeling (Figure 6) | | 70 | 70.823 | 6.49 |

of boric acid ($H_3BO_3$) as a fluoride scavenger to shift hydrolysis to the right (as portrayed in Scheme 1, eqs 1 and 2).[30−34] The hydrolyzed titanium complex ion, $[TiF_{6-n}(OH)_n]^{2-}$, leads to a hydrous oxide precipitation by condensation reactions through olation and oxolation (Scheme 1, eqs 5 and 6). The supersaturation of the solution is deliberately obtained by tuning of the feed ratio, the pH, and the temperature, and as a result, the deposition of the titanium film is initiated via the heterogeneous nucleation of titania particles on the involved surface or the attachment of preexisting titania particles.[18]

The surface phenomena of substrates play a key role in the film formation process. It is experimentally proven that a certain hydrophilic region has an affinity for $TiF_6^{2-}$, which results in the deposition of a titanium film with strong adhesive characteristics.[19−22] In contrast, the hydrophobic region repulses the aqueous molecules, resulting in either a total lack of deposition[19] or a deposition so weak that it can be peeled off from the surface by an ultrasonic lift-off.[20−22] Koumoto et al.[20−22] first modified a poly(ethylene terephthalate) (PET) surface with (3-aminopropyl)triethoxysilane (APTES) through an aminolysis reaction[35] to fabricate a silica-like surface with terminated reactive hydroxyl groups, which could initiate the formation of tolyl-terminated self-assembled monolayers (SAMs). A hydrophilic/hydrophobic hybrid surface was successfully achieved by UV photolysis of these tolyl groups by using a photomask, and subsequently, a $TiO_2$ micropattern could be obtained by LPD as a result of this large wettability contrast. Hammond et al.[23] reported a technique called polymer-on-polymer stamping (POPS) to pattern polystyrene-*b*-poly(vinylpyridine) (PS-*b*-PVP) on a poly(allylamine hydrochloride)/poly(acrylic acid) (PAH/PAA) multilayer surface. It was found that the LPD of $TiO_2$ could selectively occur on an exposed PAA region. A possible chelation between the carboxyl group in PAA and $[TiF_{6-n}(OH)_n]^{2-}$ was put forward to interpret the result. The above methods require relatively complex multistep procedures for obtaining the desired $TiO_2$ patterns on the substrate surface. Moreover, the SAM approach is limited to polyester surfaces for a reaction to occur with APTES.

Recently, a very simple hydrophilic modification method, confined photocatalytic oxidation (CPO), was developed in our group.[36] In this reaction, sulfate anion ($SO_4^-$) groups can quickly be implanted onto various polymer substrates including polyolefins, polyesters, nylons, and rubber by a routine ammonium persulfate (APS) solution followed by irradiation under UV light. As a result, a high hydrophilicity can be obtained after only a few seconds of UV irradiation. An instant idea from this reaction was to create an effective wettability pattern on the polymer surface, and a second idea was to find its application in various fabrication processes of advanced materials. A simple system

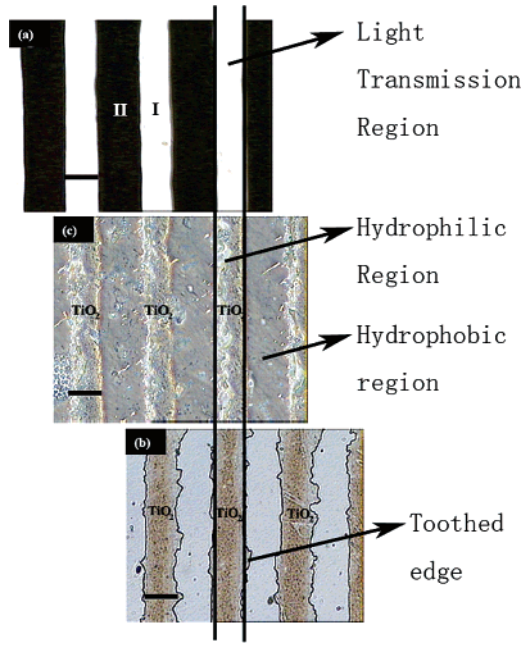


***Figure 3.*** Optical image of photomask b used with striped patterns (a). The white-colored parts (I, 50 $\mu$m) illustrate the light transmission regions, while the black parts (II, 70 $\mu$m) shield the illumination. Optical images of the positive $TiO_2$ micropattern formed on the BOPP surface after ultrasonic washing (b) and 3M Scotch adhesive tape peeling (c). The scale bars in images a−c are 50 $\mu$m.

(15) Masuda, Y.; Sugiyama, T.; Seo, W. S.; Koumoto, K. *Chem. Mater.* **2003**, *15*, 2469.
(16) Koumoto, K.; Seo, S.; Sugiyama, T.; Seo, W. S. *Chem. Mater.* **1999**, *11*, 2305.
(17) Masuda, Y.; Koumoto, K. *Langmuir* **2003**, *19*, 4415.
(18) Pizem, H.; Sukenik, C. N.; Sampathkumaran, U.; McIlwain, A. K.; Deguire, M. R. *Chem. Mater.* **2002**, *14*, 2476.
(19) Collins, R. J.; Shin, H.; DeGuire, M. R.; Heuer, A. H.; Sukenik, C. N. *Appl. Phys. Lett.* **1996**, *69*, 860.
(20) Xiang, J. H.; Masuda, Y.; Koumoto, K. *Adv. Mater.* **2004**, *16*, 1461.
(21) Zhu, P. X.; Teranishi, M.; Xiang, J. H.; Masuda, Y.; Seo, W. S.; Koumoto, K. *Thin Solid Films* **2005**, *473*, 351.
(22) Xiang, J. H.; Zhu, P. X.; Masuda, Y.; Koumoto, K. *Langmuir* **2004**, *20*, 3278.
(23) Tokuhisa, H.; Hammond, P. T. *Langmuir* **2004**, *20*, 1436.
(24) Dutschke, A.; Diegelmann, C.; Löbmann, P. *Chem. Mater.* **2003**, *15*, 3501.
(25) Pizem, H.; Gershevitz, O.; Goffer, Y.; Frimer, A. A.; Sukenik, C. N.; Sampathkumaran, U.; Milhet, X.; McIlwain, A.; De Guire, M. R.; Meador, M. A. B.; Sutter, J. K. *Chem. Mater.* **2005**, *17*, 3205.
(26) Dutschke, A.; Diegelmann, C.; Löbmann, P. *J. Mater. Chem.* **2003**, *13*, 1058.
(27) Herbig, B.; Löbmann, P. *J. Photochem. Photobiol., A* **2004**, *163*, 359.
(28) Strohm, H.; Löbmann, P. *Chem. Mater.* **2005**, *17*, 6772.
(29) Shimizu, K.; Zmai, H.; Hirashima, H.; Tsukuma, K. *Thin Solid Films* **1999**, *351*, 220.
(30) Gao, Y.; Masuda, Y.; Koumoto, K. *Chem. Mater.* **2003**, *15*, 2399.
(31) Gao, Y.; Masuda, Y.; Yonezawa, T.; Koumoto, K. *Chem. Mater.* **2002**, *14*, 5006.
(32) Yu, J. G.; Yu, H. G.; Cheng, B.; Zhao, X. J.; Yu, J. C.; Ho, W. K. *J. Phys. Chem. B* **2003**, *107*, 13871.
(33) Gao, Y.; Masuda, Y.; Peng, Z.; Yonezawa, T.; Koumoto, K. *J. Mater. Chem.* **2003**, *13*, 608.
(34) (a) Zhitomirsky, I.; Gal-Or, L.; Kohn, A.; Hennicke, H. W. *J. Mater. Sci.* **1995**, *30*, 5307.(b) Niesen, T. P.; Joachim, B.; Fritz, A. *Chem. Mater.* **2001**, *13*, 1552. (c) Jolivet, J. P.; Henry, M.; Livage, J.; Bescher, E. *Metal Oxide Chemistry and Synthesis*; John Wiley & Sons: Chichester, U.K., 1994; p 53. (d) Henry, M.; Jolivet, J. P.; Livage, J. *Struct. Bonding* **1992**, *77*, 153.
(35) Fadeev, A. Y.; McCarthy, T. J. *Langmuir* **1998**, *14*, 5586.
(36) Yang, P.; Deng, J. Y.; Yang, W. T. *Polymer* **2003**, *44*, 7157.

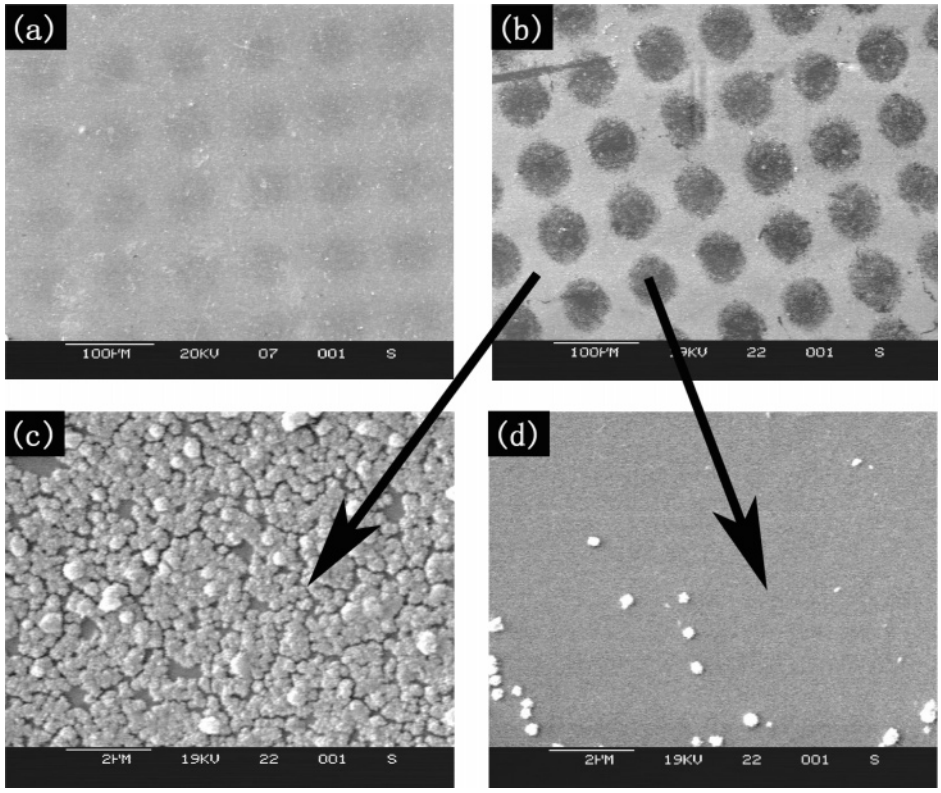


***Figure 4.*** SEM micrographs of negative patterns on the BOPP surface before (a) and after (b) ultrasonic washing and the corresponding enlarged micrographs of the hydrophobic (outside the circle, c) and hydrophilic (within the circle, d) regions.

where polyaniline was micropatterned on the treated surface by CPO gave the first example.[37] Naturally, the fabrication of inorganic materials, such as $TiO_2$, onto the surfaces of organic substrates would involve more problems than polymerization of an organic monomer such as aniline. After systemic experimental research, four novel and original results were obtained: (1) A positive $TiO_2$ micropattern with strong adhesive forces was formed on a hydrophilic region, by using a photomask that could be applied for most organic polymer substrates. (2) For the first time, by using the same photomask and carefully controlling the reaction parameters, a negative pattern (which could endure ultrasonic washing) was obtained on a hydrophobic region (Figure 1). (3) It was demonstrated that the aforementioned pattern could be used as a flexible polymer-based photomask to fabricate patterned photografting of PAA on polypropylene (PP) film surfaces. (4) Finally, the formation mechanism of the positive and negative patterns could be interpreted as the exchange of surface functionalities from sulfate to hydroxyl groups during the deposition.

## Experimental Section

**Materials.** Commercially available biaxially oriented polypropylene (BOPP) films were ultrasonically washed (80 kHz, the 100% input power was 250 W) for 15 min in a sequence of water, ethanol, and acetone and then dried in an oven before the subsequent modification. Analytical grade APS, ammonium hexafluorotitanate ($(NH_4)_2TiF_6$, chemical grade), and $H_3BO_3$ (analytical grade) were used as received. Ultrapure water was used in all experiments and was obtained by Aquapro (Shanghai, China).

**Procedures of CPO.** A thin layer of an aqueous APS solution (30 wt %) was sandwiched between two polymer films (BOPP as the top film) and exposed to UV irradiation (high-pressure mercury lamp, 1000 W; UV intensity, 8000 $\mu m/cm^2$; irradiation time, 120 s). For a wettability-patterned surface, a photomask with either a circular (Figure 2a) or a striped (Figure 3a) pattern (see also Figure S-1 in the Supporting Information) was applied on the top film (Figure 1a). A detailed description of this procedure can be found elsewhere.[36]

**$TiO_2$ Micropatterning by LPD.** The wettability-patterned film (Figure 1b) was allowed to float in a solution containing a given amount of $(NH_4)_2TiF_6$ and $H_3BO_3$ (the modified surface placed downward). For the fabrication of a positive pattern (i.e., the formation of the $TiO_2$ film on the hydrophilic region), the conditions were as follows: $(NH_4)_2TiF_6$, 0.05 M; $H_3BO_3$, 0.15 M; deposition carried out for 6 h at 50 °C (Figure 1c). For a negative pattern (i.e., the formation of the $TiO_2$ film on the hydrophobic region), the conditions were as follows: $(NH_4)_2TiF_6$, 0.05 M; $H_3BO_3$, 0.10 M; deposition lasted 3 h at 50 °C (Figure 1d). Once the deposition was finished, the as-deposited film underwent ultrasonic washing (80 kHz, the 100% input power was 250 W) in distilled water for 10 min. For the adhesive tape peeling experiment, a piece of 3M Scotch adhesive tape, Scotch crystal clear tape (Cinta Cristal, CC1920-Bx), was placed on the deposited film, pressed gently to achieve a homogeneous contact between the tape and the film, and then peeled off quickly along the length direction of the striped pattern.

**Micropatterning of BOPP by Photografting through a Negative $TiO_2$ Patterned Photomask**. A photografting polymerization solution was prepared by cosolving acrylic acid (AA) and benzophenone (BP) in acetone (AA, 10 wt %; BP, 1 wt %). A predetermined amount of the solution was sandwiched between two BOPP films using a sandwiching method similar to that of CPO. Another BOPP film onto which a negative $TiO_2$ pattern was deposited under negative conditions (Figure 1d) was placed on the top BOPP film as a photomask to micropattern the photografting regions. UV irradiation (high-pressure mercury lamp, 1000 W; UV intensity, 8000 $\mu m/cm^2$) was conducted for 1−4 min. After the irradiation step, the top and bottom BOPP films were separated, washed by copious amounts of acetone to remove

(37) Yang, P.; Xie, J.; Yang, W. *Macromol. Rapid Commun.* **2006**, *27*, 418.

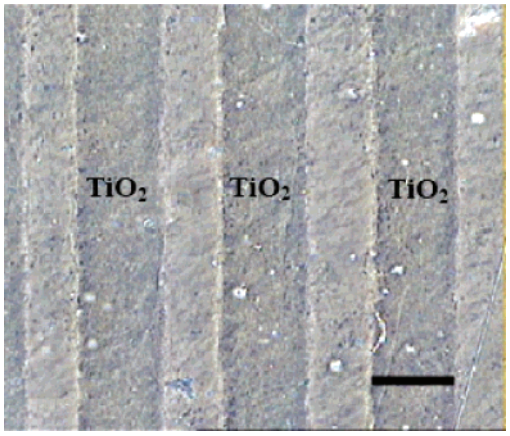


***Figure 5.*** Optical images of the negative $TiO_2$ micropattern formed on a BOPP surface (using photomask b) after ultrasonic washing. The scale bar is 70 $\mu$m.

unreacted BP, and then subjected to Soxhlet extraction with water for 8 h to remove homopolymers. To stain the grafted surface, the samples were then immersed in 1 wt % toluidine blue in a sodium phosphate buffer (0.1 M, pH 8) for 5 min,[38a] rinsed with water, and dried in an oven.

**Hydrolysis Reaction of Grafted Sulfate Groups**. As described in the text above, sulfate anion groups were introduced onto the film surface by CPO. This film was thus denoted "sulfated". These sulfate groups could further transform into hydroxyl groups by a hydrolysis reaction, and the product yield (the percentage of transformation) reached 60%. (This was calculated as the amount of transformed sulfur divided by the initial sulfur content; see the Results and Discussion). The resulting film was denoted "fully hydroxylated". A hydrolysis reaction was conducted by floating the sulfated film in ultrapure water at 30 °C or in an aqueous solution of $H_3BO_3$ (pH 3.8, 0.447 M) at 50 °C for varying amounts of time (the sulfated surface placed downward). After the reaction, the film was withdrawn and washed with water and acetone, respectively, after which it was dried in an oven (50 °C) for 5 min.

**Characterization.** Optical microscopic observations were carried out on a Nikon TE2000-s system (Tokyo, Japan). Atom force microscopy (AFM) in tapping mode was performed on a CP-II (DI Co.). UV/vis absorption spectra were recorded by a GBC Cintra 20 spectrophotometer (Australia), and XRD analysis was performed by a D/MAX 2500 VB2+/PC (Rigaku Co., Japan). Adhesion measurements were carried out using 3M Scotch adhesive tape, Scotch crystal clear tape (Cinta Cristal, CC1920-Bx). Scanning electron micrography (SEM) was performed on a S250HK3 (Cambridge). High-resolution field-emission SEM (FE-SEM) was conducted on a Sterscan 250MK3 (Cambridge). Surface contact angle measurements were performed on an OCA 20 (Dataphysics, Germany). All measurements were done at room temperature and were averages of at least six readings at different positions across the surface. Attenuated total reflection Fourier transform infrared (ATR-FTIR) spectra were recorded by a Nicolet Nexus 670 spectrometer (Thermo-Nicolet) with a 4 $cm^{-1}$ resolution, and a variable-angle ATR accessory (PIKE ATRMax II) was utilized with ZnSe as the IRE wafer. XPS spectra were obtained by using an ESCALAB 250 (VG Scientific) instrument and Al/K$\alpha$ excitation at a 45° angle. The obtained binding energy (BE) was referenced to the main carbon peak set to 285.0 eV. The atom ratio of C to O to S was given automatically by the software (provided by the manufacturer).

(38) (a) Wang, Y.; Lai, H-H.; Bachman, M.; Sims, C. E.; Li, G. P.; Allbritton, N. L. *Anal. Chem.* **2005**, *77*, 7539. (b) Hu, S.; Ren, X.; Bachman, M.; Sims, C. E.; Li, G. P.; Allbritton, N. L. *Anal. Chem.* **2004**, *76*, 1865. (c) Deng, J. P.; Yang, W. T.; Rånby, B. *J. Appl. Polym. Sci.* **2001**, *80*, 1426−1433.

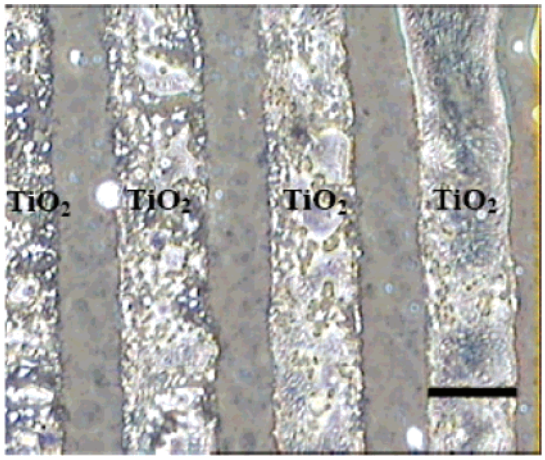


***Figure 6.*** Optical images of the negative $TiO_2$ micropattern on the adhesive tape surface (using photomask b) fabricated by the 3M Scotch adhesive tape peeling. The scale bar is 70 $\mu$m.

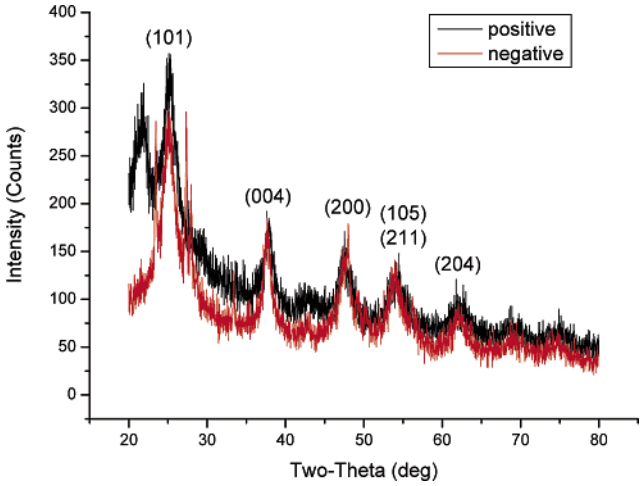


***Figure 7.*** XRD patterns of powder removed from deposited films: deposition on the hydrophilic surface under positive patterning conditions (black curve) and deposition on the hydrophobic surface under negative patterning conditions (red curve).

## Results and Discussion

**Positive Patterns.** When the hydrophilic/hydrophobic patterned BOPP was allowed to come in contact with the LPD reaction solution, the deposition occurred simultaneously on the hydrophilic/hydrophobic regions, as shown in Figure 2b. However, ultrasonic washing would peel off the weakly bonded deposition on the hydrophobic regions to give out a positive pattern obtained from the photomask (Figure 2a). By optimizing the reaction conditions through extensive comparison and parallel experiments, we thus found that the best positive pattern was obtained by employing the positive conditions described in Figure 1c. The optical image in Figure 2c portrays a typical positive pattern from the as-deposited $TiO_2$ film after ultrasonic lift-off. The thickness, as measured by AFM analysis, was 350 nm. A 3D AFM profile image (Figure 2d) showed that the microscopic structure of the $TiO_2$ deposition consisted in dense column arrays and the resulting fusions which should be attributed to the preferential *c* axis (normal line direction on the surface) orientated crystallization growth of $TiO_2$.[15,24,28]

Line edge variation is an important parameter for fabricating electronic microstructures. To simplify the calculation, photo-

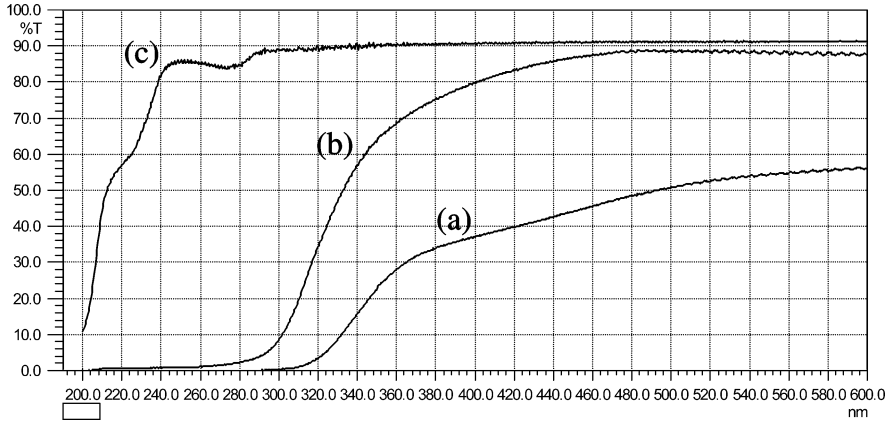


***Figure 8.*** UV−vis spectra of the film deposited under positive and negative conditions: (a) the film formed on the hydrophilic BOPP surface under positive conditions; (b) the film formed on the hydrophobic BOPP surface under negative conditions; (c) an unmodified BOPP film.

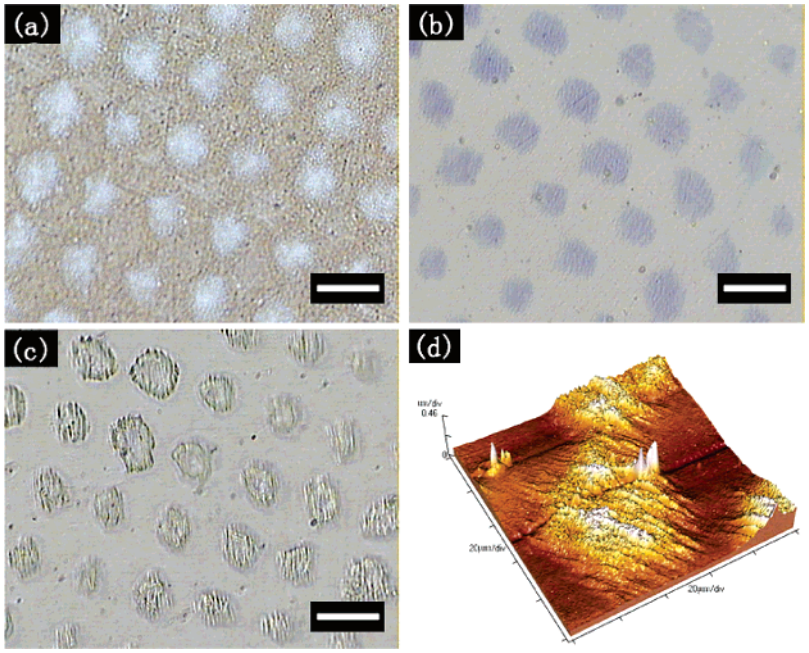


***Figure 9.*** Micropatterning of a BOPP surface using the negative $TiO_2$ pattern on the BOPP film as a photomask: (a) phase contrast microscope image of the negative $TiO_2$ pattern on the BOPP film; (b) optical microscope image of the patterned PAA grafts on the BOPP surface after staining with toluidine blue (the irradiation time was 1 min); (c) phase contrast microscope image of the patterned PAA grafts on the BOPP surface (the irradiation time was 3 min); (d) 3D AFM image of a circle from the PAA grafted region on the BOPP surface (the irradiation time was 3 min). The scale bars in images a−c are 80 $\mu$m.

mask b with a striped pattern was used (Figure 3a), and the obtained deposition film after ultrasonic washing is shown in Figure 3b. A striped $TiO_2$ film with a toothed edge and wider stripes than for photomask b can be seen. As an example, it can be mentioned that an average stripe width of 56 $\mu$m was obtained as opposed to 50 $\mu$m for the photomask (Table 1). The resulting line edge variation for the positive pattern was 17%. This value was lower than what is usually seen for SAM-modified surfaces with similar lift-off processes (28%)[16] but exceeds the usual 5% variation accepted by current electronics design rules. Recently, seed layer[17] and barrier effect[20] processes have been utilized to improve the line edge acuity on the SAM-modified surface to 2.1%. When a 3M Scotch adhesive tape peeling was carried out, a more regular $TiO_2$ stripe with a 49 $\mu$m width remained. The resulting line edge variation was reduced to 4.8% (Figure 3c). These results show that the toothed $TiO_2$ parts on the hydrophobic region could endure the ultrasonic washing as a result of their fusion bonding with parts on the hydrophilic region but that they could not survive the peeling-off force from the adhesive tape. Obviously, this approach not only provided a simple and low-cost method to fabricate the applicable micropatterned $TiO_2$ film without the use of seed or barrier layers but also proved a very good affinity of the $TiO_2$ film for the CPO-treated surface.

***Table 2.*** Changes in pH during LPD under Positive and Negative Conditions

| | positive deposition conditions | | negative deposition conditions | |
|---|---|---|---|---|
| time (h) | hydrophilic surface | hydrophobic surface | hydrophilic surface | hydrophobic surface |
| 0 | 3.78 | 3.78 | 3.76 | 3.76 |
| 1 | 3.715 | 3.745 | 3.72 | 3.735 |
| 3 | 3.65 | 3.65 | 3.65 | 3.695 |
| 6 | 3.62 | 3.62 | 3.625 | 3.63 |
| 9 | 3.61 | 3.55 | 3.64 | 3.65 |
| 12 | 3.64 | 3.65 | 3.670 | 3.65 |

Since the CPO method can be conducted on the surfaces of most organic polymers,[36] we believe that this fabricating method to obtain positive patterns is, apart from being simple, of low-

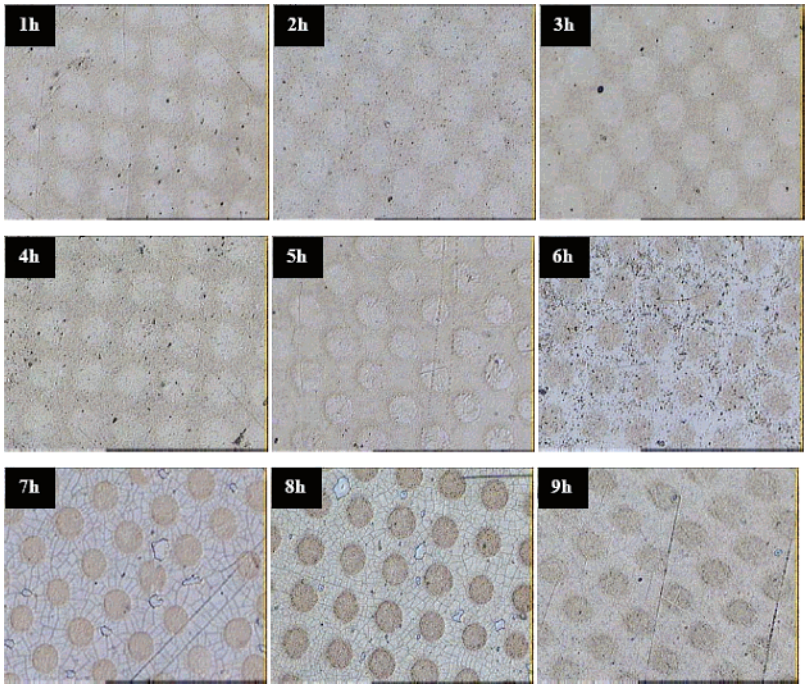


***Figure 10.*** Time-resolved evolution process of the $TiO_2$ pattern on the wettability-patterned BOPP surface under positive deposition conditions. In these optical photos, the arrays of circles show the hydrophilic regions modified by CPO, whereas the original polymer surface maintains its hydrophobic nature. In the time range of 1−3 h, the deposition was very weak and mainly took place on the hydrophobic skeleton, forming a negative pattern (stage 1). The deposition on the hydrophilic region became increasingly apparent after 4 h (stage 2), and the optimized positive pattern was obtained at 6 h (see also Figure 2c). In the time range of 7−9 h, depositions on both the hydrophilic and hydrophobic surfaces were apparent (stage 3), and the deposition selectivity based on the wettability of the surface was diminished.

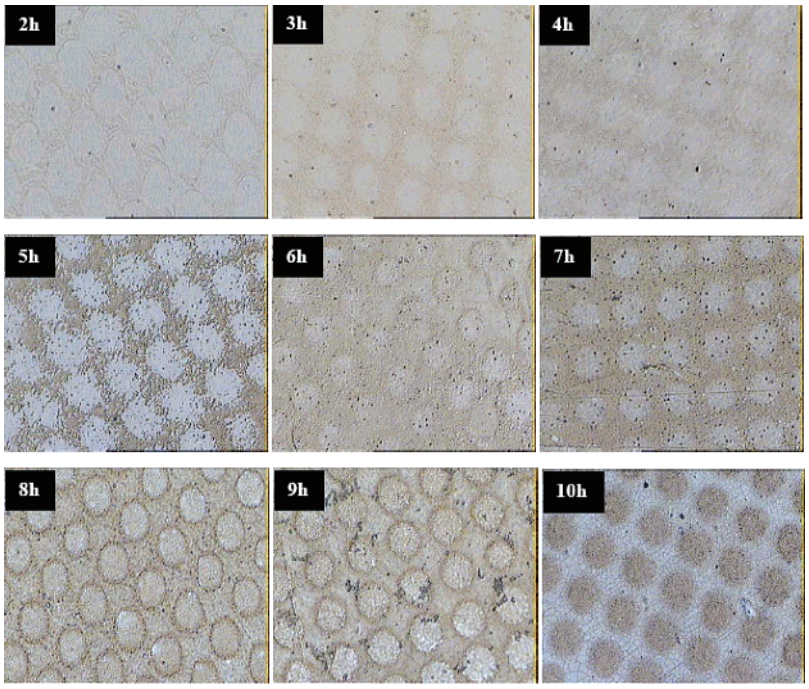


***Figure 11.*** Time-resolved evolution process of the $TiO_2$ pattern on a wettability-patterned BOPP surface under negative deposition conditions. All the photos are optical microscopy images. Up to 5 h, the deposition was very weak and mainly took place on the hydrophobic skeleton to form a negative pattern (stage 1). An optimized negative pattern was obtained after 3 h (see also Figure 4b). The deposition on the hydrophilic region became increasingly obvious after 6 h (stage 2).

cost, and inherent of strong adhesive forces, also a versatile procedure for the preparation of microstructural $TiO_2$ films on a variety of polymer surfaces. Partial results are given in Figure S-2 (Supporting Information). We nonetheless point out that it is possible that the deposition conditions need to be further optimized to obtain an enhanced pattern when the polymer substrate type is altered.

**Negative Patterns.** In a series of experiments to determine the conditions surrounding the positive $TiO_2$ patterning, we accidentally observed the occurrence of a negative pattern with

***Scheme 2.*** Chemical Exchange of the Functional Groups on the Oxidized Surface by a Hydrolysis Reaction[a]

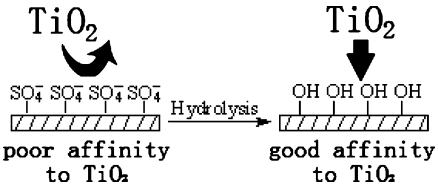


[a] It was found that the sulfate groups had poor affinity for the titanium layer ($TiO_2$), while the affinity for the hydroxyl groups was good (vide infra).

ultrasonic washing. After extensive and systematical experiments, we could conclude that the negative micropattern could be conveniently and reproductively fabricated through a simple adjustment of the feed ratio of $H_3BO_3$ to $(NH_4)_2TiF_6$ in solution from 3:1 to 2:1 as well as a shortening of the deposition time from 6 to 3 h (i.e., negative conditions in Figure 1d). The as-deposited $TiO_2$ film before ultrasonic washing consisted of a coexisting $TiO_2$ layer on both hydrophilic (irradiated) and hydrophobic (unirradiated) regions (Figure 4a). However, once the as-deposited film underwent ultrasonic washing, the $TiO_2$ layer on the hydrophilic region was peeled off whereas the $TiO_2$ layer on the hydrophobic region remained (Figure 4b). This result showed that the bonding strength of the layer on the hydrophobic region was higher than that on the hydrophilic region, a very unusual result as compared to what can be found in the present literature. Enlarged SEM images showed that the $TiO_2$ layer formed on the hydrophobic region consisted of large particles, most of which were fused together to form a continuous deposition layer, while few particles remained on the hydrophilic region (Figure 4c,d). This negative micropattern turned out to be an interconnected network with a thickness of approximately 80 nm as measured by AFM.

For the samples where photomask b was employed, the line edge variation of the negative pattern was calculated as being close to 1.45% (Figure 5)—a value lower than the 2.1% obtained for the SAM-modified surface[17,20] as well as the usual 5% variation in the current electronics design. In addition to BOPP, the negative pattern could also be fabricated on other polymer surfaces under equivalent conditions (Figure S-3, Supporting information). These results demonstrate that, by utilizing LPD and sequential ultrasonic washing, it is possible to obtain a negative pattern with improved line edge variations on a variety of polymer surfaces. When a similar 3M Scotch adhesive tape peeling was conducted on an as-deposited negative $TiO_2$ patterned film, it was found that the negative micropattern after ultrasonic washing could be completely transferred onto the adhesive tape (Figure 6), leaving no negative micropattern to remain on the substrate. Such a preparation and transfer procedure constitutes a facile method for the transfer of an inorganic microstructure with a reliable stability onto organic polymeric substrates—a hot subject in solar-cell and electronic applications at the present time.[39]

The crystallization character of patterned positive and negative depositions was analyzed by small-incidence XRD where the pattern assigned to the anatase phase was revealed (Figure 7). The (101) signal (and not the (004) signal as would have been expected) displayed the strongest intensity among the signal arrays from all crystal faces. However, this did not conflict with the aforementioned column morphology because the powder sample lost all of its crystallization structure vertical to the surface, and only average information from the randomly dispersed crystalline particles could be obtained. In fact, the pillar crystallization growth has been well confirmed by grazing-incidence XRD, where the crystallization direction of a $TiO_2$ deposition layer obtained under conditions similar to ours was investigated in situ without the need for detaching the deposition layer from the surface. These results showed a dominant intensity of the (004) signal in the entire XRD pattern.[24,25]

In fact, the negative pattern obtained from photomask a is an interconnected $TiO_2$ network coated onto the BOPP film. Potential applications are a variety of lithography masks, and in the present paper we only provide an example of a photomask. Figure 8 shows the UV−vis spectra of an unmodified BOPP film (a control sample) and two as-deposited films with different thicknesses obtained from positive (350 nm) and negative (80 nm) deposition conditions. The results reveal that the titania film deposited on the BOPP surface has a very strong absorption in the range of 200−300 nm (near 100%). This performance of the as-formed $TiO_2$ implied that photomask a could be copied (for far-UV light) onto a flexible plastic film. Such a low-cost photomask has its own advantage to be able to come into intimate contact with a solid surface as a result of its flexibility and would find an application in, for instance, curve surface photolithography. We successfully achieved patterned surface photografting of PAA on a BOPP film by using such a photomask. The acetone solution of BP and AA was sandwiched between two BOPP films, and a third BOPP film with the negative $TiO_2$ micropattern fabricated with photomask a (Figure 9a) was placed on top of this setup to control the irradiation regions. As a photosensitizer, BP could initiate the photografting of AA on the polymer surface when it was photoexcited.[38] After UV irradiation for a certain period of time, patterned PAA grafts could be directly observed by phase contrast microscopy (Figure 9c) or stained with toluidine blue, giving rise to a blue circular pattern (Figure 9b) when viewed by optical microscopy. The diameter of the circles, as measured by 3D AFM imaging (Figure 9d), was about 43 $\mu$m and thus close to the average feature (40 $\mu$m) of the negative $TiO_2$ pattern in Figure 9a.

Photomask a was a circlar metal foil with a diameter of about 6 mm, so a large deposited surface area ($mm^2$) could be obtained, as observed in our experiments. A possible application when the negative pattern forms a large area ($mm^2$) macroporous film is that such anatase titanium films play a crucial role in $TiO_2$-based applications such as microfluidics,[40] solar cells,[41] photocatalysis,[42] and lithium batteries.[43] Such interconnected patterns are for the time being impossible to obtain by traditional

(39) (a) Sun, Y.; Khang, D.-Y.; Hua, F.; Hurley, K.; Nuzzo, R. G.; Rogers, J. A. *Adv. Funct. Mater.* **2005**, *15*, 30. (b) Lee, K. J.; Motala, M. J.; Meitl, M. A.; Childs, W. R.; Menard, E.; Shim, A. K.; Rogers, J. A.; Nuzzo, R. G. *Adv. Mater.* **2005**, *17*, 2332. (c) Menard, E.; Lee, K. J.; Khang, D.-Y.; Nuzzo, R. G.; Rogers, J. A. *Appl. Phys. Lett.* **2004**, *84*, 5398. (d) Menard, E.; Nuzzo, R. G.; Rogers, J. A. *Appl. Phys. Lett.* **2005**, *86*, 093507. (e) Sun, Y.; Rogers, J. A. *Nano Lett.* **2004**, *4*, 1953.
(40) Narazaki, A.; Kawaguchi, Y.; Niino, H.; Shojiya, M.; Koyo, H.; Tsunetomo, K. *Chem. Mater.* **2005**, *17*, 6651.
(41) (a) Benkö, G.; Skårman, B.; Wallenberg, R.; Hagfeldt, A.; Sundström, V.; Yartsev, A. P. *J. Phys. Chem. B* **2003**, *1−7*, 1370. (b) Gratzel, M. *Nature* **2001**, *414*, 338. (c) Gräzel, M.; Hagfeldt, A. *Chem. Rev.* **1995**, *95*, 45. (d) Cheng, Y. J.; Gutmann, J. S. *J. Am. Chem. Soc.* **2006**, *128*, 4658.
(42) (a) Diebold, U. *Surf. Sci. Rep.* **2003**, *48*, 53. (b) Ho, W.; Yu, J. C.; Yu, J. *Langmuir* **2005**, *21*, 3486. (c) Zhang, Y.; Ebbinghaus, S. G.; Weidenkaff, A.; Kurz, T.; Nidda, H. A. K.; Klar, P. J.; Güngerich, M.; Reller, A. *Chem. Mater.* **2003**, *15*, 4028.
(43) Kavan, L.; Rathousk'y, J.; Gra1tzel, M.; Shklover, V.; Zukal, A. *J. Phys. Chem. B* **2000**, *104*, 12012.

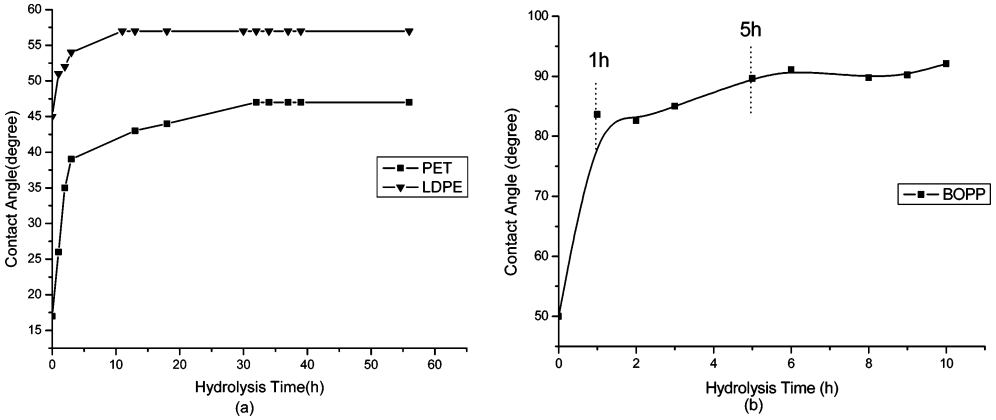


***Figure 12.*** Change in the contact angles of water on the polymer surfaces with varying soaking time for the modified polymer films in two types of aqueous solutions: (a) modified PET and LDPE samples in ultrapure deionized water at 21 °C; (b) a modified BOPP sample in an aqueous solution of $H_3BO_3$ with a pH of 3.8 at 50 °C (0.447 M).

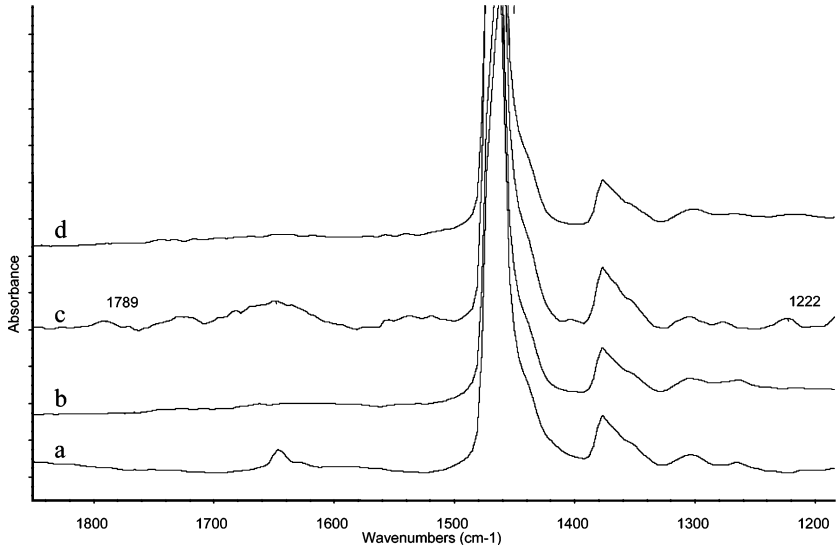


***Figure 13.*** ATR-FTIR spectra: (a) LDPE, unirradiated; (b) LDPE, irradiated; (c) derivation of modified LDPE, irradiated, soaked in water for 14 h, and then treated with TFAA; (d) derivation of modified LDPE, irradiated, treated with TFAA, and then dried under reduced pressure at 20 °C for 24 h. (The TFAA derivation conditions implied soaking the irradiated LDPE films in TFAA in a sealed tube for 40 min at 35 °C, taking them out, soaking them in ethyl ether for at least 3 h, washing them with ethyl ether, ethanol, water, and acetone in that order, and drying them under reduced pressure at 20 °C for at least 24 h.)

positive LPD methods.[15−17,19−23] The potential method proposed here does not require photoresists, templates, or high temperatures,[44,45] thereby displaying its simplicity for easy handling. The pore surface (i.e., the naked polymer region) on the substrate can be conveniently functionalized by well-founded postgrafting.[38] The resulting organic−inorganic hybrid network may provide advantages for functional, rapid-response devices.[46] Most of all, the ordered texture could be controlled with precision and tuned simply by designing the pattern of a photomask used, providing an opportunity to fabricate tailor-made functional materials with a great flexibility in their design.

**Pattern Formation Mechanism.** The mechanism behind the deposition of $TiO_2$ on hydrophilic surfaces has been extensively examined and reported in the literature.[18,26,47,48] Two main opinions have been developed, including heterogeneous nucleation to initiate crystallization growth and direct attachment of homogeneous particles in solution onto the surface. A column growth pattern in the positive patterns from the present study showed that the former seemed to dominate the positive deposition process.

The formation of a negative pattern, on the other hand, is a novel phenomenon not formerly presented, and an investigation of the mechanism behind it should be carried out. Up until now, it has been generally believed that the deposition of titanium

(44) (a) Kresge, C. T.; Leonowicz, M. E.; Roth, W. J.; Vartuli, J. C.; Beck J. S. *Nature* **1992**, *359*, 710; Beck, J. S. (b) Vartuli, J. C.; Roth, W. J.; Leonowicz, M. E.; Kresge, C. T.; Schmitt, K. D.; Chu, C. T.-W.; Olson, D. H.; Sheppard, E. W.; McCullen, S. B.; Higgins, J. B.; Schlenker, J. L. *J. Am. Chem. Soc.* **1992**, *114*, 10834. (c) Huo, Q.; Margolese, D. I.; Ciesla, U.; Demuth, D. G.; Feng, P.; Gier, T. E.; Sieger, P.; Firouzi, A.; Chmelka, B. F.; Schüth, F.; Stucky, G. D. *Chem. Mater.* **1994**, *6*, 1176. (d) Zhao, D.; Feng, J.; Huo, Q.; Melosh, N.; Fredrickson, G. H.; Chmelka, B. F.; Stucky, G. D. *Science* **1998**, *279*, 548. (e) Zhao, D.; Huo, Q.; Feng, J.; Chmelka, B. F.; Stucky, G. D. *J. Am. Chem. Soc.* **1998**, *120*, 6024. (f) Yang, P.; Zhao, D.; Margolese, D. I.; Chmelka, B. F.; Stucky, G. D. *Nature* **1998**, *395*, 583. (g) Yang, P.; Zhao, D.; Margolese, D. I.; Chmelka, B. F.; Stucky, G. D. *Chem. Mater.* **1999**, *11*, 2813. (h) Brinker, C. J.; Lu, Y. F.; Sellinger, A.; Fan, H. Y. *Adv. Mater.* **1999**, *11*, 579.

(45) (a) Smarsly, B.; Grosso, D.; Brezesinski, T.; Pinna, N.; Boissière, C.; Antonietti, M.; Sanchez, C. *Chem. Mater.* **2004**, *16*, 2948. (b) Crepaldi, E. L.; Soler-Illia, G. J. de A. A.; Grosso, D.; Cagnol, F.; Ribot, F.; Sanchez, C. *J. Am. Chem. Soc.* **2003**, *125*, 9770. (c) Grosso, D.; Soler-Illia, G. J. de A. A.; Crepaldi, E. L.; Cagnoi, F.; Sinturel, C.; Bourgeois, A.; Bruneau, A. B.; Amenitsch, H.; Albouy, P. A.; Sanchez, C. *Chem. Mater.* **2003**, *15*, 4562.

(46) Fuertes, M. C.; Soler-Illia, G. J. A. A. *Chem. Mater.* **2006**, *18*, 2109.

(47) Niesen, T. P.; De, Guire, M. R. *J. Electroceram.* **2001**, *6*, 169.

(48) Yang, H. G.; Zeng, H. C. *J. Phys. Chem. B* **2003**, *107*, 12244.

***Table 3.*** Elemental Analysis of S and O from XPS Measurements on a Hydrolyzed BOPP Surface[a]

| time (h) | S | O | time (h) | S | O |
|---|---|---|---|---|---|
| 0 | 0.68−0.83 | 13.75 | 5 | 0.31 | 4.91 |
| 1 | 0.44 | 7.55 | 8 | 0.38 | 4.66 |
| 2 | 0.37 | 6.59 | 9 | 0.31 | 4.03 |

[a] Hydrolysis conditions: concentration of $H_3BO_3$ 0.447 M, pH 3.8, 50 °C.

films with strong adhesive characteristics could only be obtained on hydrophilic polymer surfaces. The deposition on hydrophobic surfaces, although readily obtainable, leads to an adhesion so weak that the layer is easily peeled off.[24,28] Löbmann et al.[24] have reported that a high hydrophilicity was unnecessary for the deposition of a $TiO_2$ layer. This statement was based on the finding that a continuous film could be formed on an untreated PS surface. However, they further found that a satisfactory adhesion only existed on hydrophilically modified PS surfaces, whereas $TiO_2$ films on untreated surfaces were easy to peel off with a sharp water jet. Pizem et al.[18] found that, under the same deposition conditions, only one of the silanol-bearing and sulfonated silica surfaces could support the growth of a continuous and uniform film while the other did not. Some changes of pH, molarity, and temperature in the deposition conditions could reverse this effect of the substrate. They attributed this result to a change of the electrostatic attraction between modified silica surfaces and $TiO_2$ particles in the solutions. Masuda et al. also expressed an electrostatic interaction-induced deposition mechanism on amino-terminated SAM-modified silica surfaces.[15]

In our system, the influence of pH was first excluded. Under both conditions, the pH was initially 3.78. As the reactions advanced under the two types of deposition conditions, the pH in the reaction solution did not undergo any drastic changes (Table 2). We thus carried out time-resolved deposition topography investigations under positive (Figure 10) and negative (Figure 11) conditions. The darker part in optical microscopy presented a titania deposited region while the brighter regions were assigned to a BOPP film surface with little or less deposition. From the observations, one could find that whether under positive or negative conditions, the pattern had undergone a negative-to-positive (n−p) transformation. Under positive conditions, the pattern presented a subtle negative deposition on the hydrophobic surface with the hydrophilic region more or less undisturbed from 1 to 3 h (stage 1). The deposition on the hydrophilic regions became increasingly apparent after 3 h (stage 2), and the obvious n−p transformation took place after 5 h. When the deposition time increased to 6 h, the optimized positive pattern was formed with a low amount of deposition on the hydrophobic surface (see also Figure 2c). In contrast, negative conditions used a lower amount of $H_3BO_3$ than that in the positive solution, and the pattern at 1 h under negative conditions was thus not observable due to a lower extent of supersaturation of the solution and the resulting very small deposition amount. Instead, a negative pattern was observed from 2 h lasting to 5 h with no or slight deposition on the hydrophilic regions (stage 1). After that, the n−p transformation also took place. Accordingly, we found that both conditions held the same n−p transformation time point, 5 h, which was denoted $T_{np}$. After $T_{np}$, the depositions on the hydrophobic region became evident (stage 3, 7−9 h, and stage 2, 6−10 h, for positive and negative conditions, respectively), and the pattern increasingly displayed a coexistence of depositions on both the hydrophilic and hydrophobic surfaces, which showed that the selectivity of wettability-determined deposition was diminished.

The similar deposition evolution under positive or negative conditions made us consider that there may be some conjunct reasons for the pattern deposition. Pizem et al.[25] pointed out that during the LPD process reactive imide groups contained in the polyimide (PMR-15) surface could be partially hydrolyzed because of the acidic oxide deposition solution. As a result, carboxyl groups were formed to allow adhesion of the titania film through chelation between the exposed carboxyl groups and titanium ions. Inspired by their report, we paid attention to the change in chemical structure of the polymer surface during the two types of deposition. We found the implanted sulfate anion groups after CPO reaction were transformed into hydroxyl groups by simply soaking the surface in water, after which the exchange of surface functionalities directly affected the deposition pattern due to the difference in affinity between the sulfate and hydroxyl groups as opposed to the $TiO_2$ particles (Scheme 2).

This hydrolysis reaction was supported by the following evidence. First, the treated films were soaked in water at 21 °C, a procedure that led to the contact angle of water (CA) on the treated film surfaces (PET, low-density polyethylene (LDPE), and BOPP) to increase slowly with a prolonged dipping time before leveling off (Figure 12). It has been reported that polymer surfaces hydrophilized by oxidizing treatments should not decay when stored in water or high-energy media,[49] which was apparently in conflict with the results displayed in Figure 12. It was considered that the difference in surface free energy between the sulfate anion and hydroxyl implanted surfaces resulted in the continuous increase of the CA on the treated surface. When the hydrolysis reached an equilibrium, the CA values became constant, which was mainly due to the hydrophilicity of the hydroxyl groups and not the sulfate anion groups before soaking. Second, this judgment could be strongly supported by Figure 13. Samples before and after soaking were derivatized with trifluoroacetic anhydride (TFAA).[50] Subsequent investigation by ATR-FTIR was a means of obtaining an indication of the hydroxyl groups on surfaces since the esterification between the hydroxyl groups and TFAA would be apparent in the ATR-FTIR spectra. The spectrum of the sample after soaking (c) displayed an ester carbonyl bond at 1789 $cm^{-1}$ and a C−F bond at 1222 $cm^{-1}$, both of which could not be found in the spectra of the sample before soaking (b, d) nor for the untreated LDPE (a). This further illustrated that, before soaking, the polar groups on the treated surface were not mainly hydroxyl but sulfate groups while, after soaking, the sulfate groups were hydrolyzed and transformed into hydroxyl groups, which could easily react with TFAA.

It is possible that the hydrolysis process started when the aqueous LPD reaction took place. We found that at a pH similar

(49) (a) Hoffman. A. S. *Macromol. Symp.* **1996**, *101*, 443−454. (b) Bergbreiter, D. E. *Prog. Polym. Sci.* **1994**, *19*, 529. (c) Singh. R. P. *Prog. Polym. Sci.* **1992**, *17*, 251.
(50) (a) Price, G. J.; Keen, F.; Clifton, A. A. *Macromolecules* **1996**, *29*, 5664. (b) Kubota, H.; Hariya, Y.; Kuroda, S.; Kondo, T. *Polym. Degrad. Stab.* **2001**, *72*, 223. (c) Lee, K. W.; McCarthy, T. J. *Macromolecules* **1988**, *21*, 209.

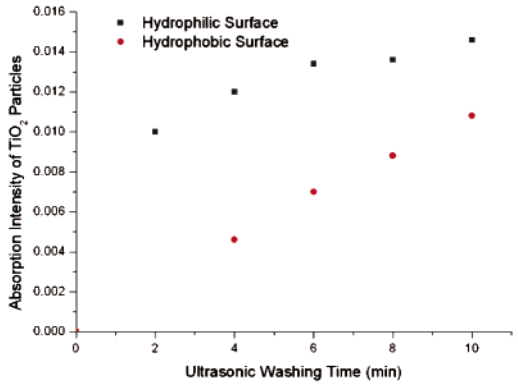


***Figure 14.*** Peeling kinetics during ultrasonic washing. After the hydrophilic (black squares) and hydrophobic (red circles) surfaces underwent LPD under negative conditions, a higher peeling speed was observed on the hydrophilic surface during the ultrasonic washing. The amount of peeled $TiO_2$ was reflected by recording the UV absorption intensity (at 300 nm) of the ultrasonic washing solution.

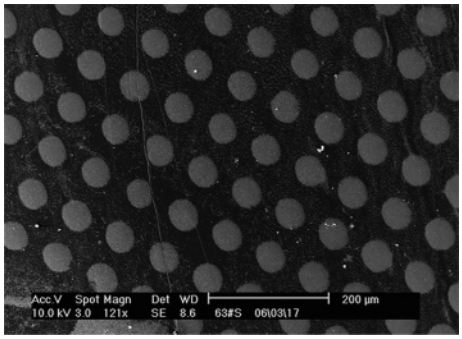


***Figure 15.*** An FE-SEM micrograph of a patterned $TiO_2$ deposition on a hydroxylated BOPP surface under negative conditions. From the image it can be seen that a positive $TiO_2$ pattern was formed (i.e., the deposition layer was preferentially attached to the hydrophilic modified surface), although under the same conditions a negative pattern was formed on the sulfated surface.

to that in the $TiO_2$ deposition reaction, the CA values on the sulfated surface increased due to the advancement of the hydrolysis reaction (Figure 12b). The main kinetic character was found to increase rapidly for the first hour before reaching a maximum value near 5 h, which was in accordance with the $T_{np}$ in the above deposition evolution. The existence of such kinetics was further proved by elemental analysis from XPS on the corresponding surfaces (Table 3). At 1 h, the initial amount of sulfur had decreased to a large extent as the transformation into hydroxyl groups took place. This transformation speed slowed between 1 and 5 h and changed slightly afterward. By dividing the amount of decreased S by the initial S content, the transmission percentage was found to approach 60%. The amount of oxygen decreased steadily due to the loss of oxygen atoms as the sulfate groups transformed into hydroxyl groups. Therefore, we could clearly find that the hydrolysis kinetics and the corresponding XPS evidence agreed well with the time-resolved evolution process of the $TiO_2$ pattern whether under positive or negative conditions. These experimental results encouraged us to put forward a hydroxyl-dependent pattern evolution mechanism.

A direct consideration is that the newly formed hydroxyl groups are more favorable to the deposition of the $TiO_2$ layer than the sulfate groups (Scheme 2) as a result of the hydroxyl groups being known to favor the deposition of $TiO_2$ whether on silicon[15,18] or on polymer surfaces (PS).[24] A possible reason for this is that surface hydroxyl groups could take part in the condensation polymerization among $Ti(OH)_6^{2-}$ to form a supported Ti−O−Ti network structure (Scheme 1). In contrast, it seemed possible that there was a poor affinity between the sulfate anion groups and the $TiO_2$ particles because of an electrostatic repulsion force. The pH in our reaction system was around 3.78, which was a little higher than the low limit (∼3) of the isoelectric point range (∼3−7.5) of $TiO_2$ particles reported in the literatures.[51] It was thus possible that the particles were a little negatively charged. This was further supported by Masuda et al., who detected the negative $\xi$ potential on the $TiO_2$ surface as −20 mV at a pH of 3.8, due to the adsorption of solvated anion groups to the particle surface.[15] The poor affinity could be supported further by the peeling kinetics during the ultrasonic washing. The $TiO_2$ particles formed under negative deposition conditions were peeled off from the sulfated (hydrophilic) and original (hydrophobic) surfaces and dispersed into the ultrasonic washing solution. The UV absorption intensity of the solution containing the $TiO_2$ particles was in proportion to the amount of $TiO_2$ particles in the solution. We found that the peeling speed on the hydrophilic sulfated surface was higher than that on the hydrophobic surface (Figure 14).

Accordingly, the evolution process during both depositions could be reinterpreted on the basis of the hydrolysis kinetics. The poor affinity from sulfate anion groups directly resulted in few $TiO_2$ layers remaining on the hydrophilic region after ultrasonic washing at the initial deposition stage, while the hydrolysis of the sulfate groups provided the hydrophilic region with a chance to increase the surface concentration of the hydroxyl groups with a higher affinity for $TiO_2$. As a result, an n−p transformation took place as observed in Figures 10 and 11. For instance, under positive conditions, the pattern initially presenting the subtle, negative deposition took place on the hydrophobic surface with the sulfated hydrophilic region undisturbed (stage 1, 1−3 h). As the deposition time increased, hydroxylation on the hydrophilic region took place to a larger extent, and this increased hydroxylation further facilitated the $TiO_2$ deposition on the surface (stage 2, 4−6 h). When the deposition time increased to 6 h, the optimized positive pattern was formed with a low deposition amount on the hydrophobic surface. The deposition in the last stage displayed obvious pollution of the hydrophobic surface, which came from the very long deposition time (stage 3, 7−10 h). To further support this deduction, we deliberately placed the fully hydroxylated surface into the negative deposition system and found that, after the same deposition time (3 h), a positive pattern was formed (Figure 15), which strongly indicated hydroxyl groups were "more attractive" to the titanium layer as they induced the formation of a positive pattern on the surface.

(51) (a) Nadtochenko, V.; Denisov, N.; Sarkisov, O.; Gumyc, D.; Pulgarin, C.; Kiwi, J. *J. Photochem. Photobiol., A* **2006**, *181*, 401. (b) Kosmulski, M.; Rosenholm, J. B. *Colloids Surf., A* **2004**, *248*, 121; *J. Phys. Chem.* **1996**, *100*, 11681. (c) Dumont, F.; Warlus, J.; Watillon, A. *J. Colloid Interface Sci.* **1990**, *138*, 543. (d) Furlong, D. N.; Parfitt, G. D. *J. Colloid Interface Sci.* **1978**, *65*, 548. (e). Parfitt, G. D. *Prog. Surf. Membr. Sci.* **1976**, *11*, 181. (f) Larson, I.; Drummond, C. J.; Chan, D. Y. C.; Grieser, F. *J. Am. Chem. Soc.* **1993**, *115*, 11885. (g) Tschapek, M.; Wasowski, C.; Torres, Sanchez, R. M. *J. Electroanal. Chem.* **1976**, *74*, 167. (h) Sene, J. J.; Zeltner, W. A.; Anderson, M. A. *J. Phys. Chem. B* **2003**, *107*, 1597.

## Summary and Conclusions

In conclusion, we have developed a very simple method to create positive and negative $TiO_2$ micropatterns on a wettability-patterned polymer surface. A positive pattern provided an effective and versatile solution toward inert polymer substrates, while a negative pattern refuted the conventional opinion that a hydrophilic region would favor the formation of a $TiO_2$ film. This helped us obtain a patterned $TiO_2$ film on a pristine (hydrophobic) polymer surface. The gradual transformation of the sulfate functionalities into hydroxyl groups during the deposition process led to a change in the affinity on the modified surface and resulted in a change in the pattern type from the initial negative pattern (the hydrophilic sulfated region weakened the deposition) to a positive one (the newly formed hydroxyl on sulfate modified region facilitated the deposition). Such a negative pattern facilitates the fabrication of an interconnected $TiO_2$ micronetwork and flexible photomasks with reliable stabilities on common, original, or adhesive-coated hydrophobic plastic surfaces. The former could be a crucial framework in providing a host space for further nanoparticle incorporation or enhanced electron transport,[30,31,52−56] while the latter was exemplified by patterned photografting of PAA on a BOPP film surface using such a polymer-based photomask. Our work offers a photoresist-free opportunity for fabricating positive and negative patterns on a flexible substrate by using just one photomask. The resulting complementary patterns may effectively modify the product property or fabricate novel electrooptical devices if various nanoparticles,[52−54] photosensizers,[52] or complex salts[30,31] are incorporated into the negative film.

**Acknowledgment.** We acknowledge funding of the Major Project (Grant 50433040) from the National Natural Science Foundation of China (NSFC) and the Major Project (Grants XK100100433 and XK100100540) for Polymer Chemistry and Physics Subject Construction from the Beijing Municipal Education Commission (BMEC).

**Supporting Information Available:** Optical images of positive and negative $TiO_2$ micropatterns on additional polymer substrates aside from BOPP (Figures S-1−3). This material is available free of charge via the Internet at http://pubs.acs.org.

JA063716O

(52) Li, X. S.; Fryxell, G. E.; Birnbaum, J. C.; Wang, C. *Langmuir* **2004**, *20*, 9095.
(53) Pérez, M.; Otal, E.; Bilmes, S. A.; Soler-Illia, G. J. A. A.; Crepaldi, E. L.; Grosso, D.; Sanchez, C. *Langmuir* **2004**, *20*, 6879.
(54) Yu, C.; Tian, B.; Zhao, D. *Curr. Opin. Solid State Mater. Sci.* **2003**, *7*, 191.
(55) Deki, S.; Aoi, Y.; Yanagimoto, H.; Ishii, K.; Akamatsu, K.; Mizuhata, M.; Kajinami, A. *J. Mater. Chem.* **1996**, *6*, 1879.
(56) Adachi, M.; Murata, Y.; Takao, J.; Jiu, J.; Sakamoto, M.; Wang, F. *J. Am. Chem. Soc.* **2004**, *126*, 14943.